Drug–Polymer Interactions in Hydrogel-based Drug-Delivery Systems: An Experimental and Theoretical Study

Filippo Rossi,*[a] Franca Castiglione,[a] Monica Ferro,[a] Paolo Marchini,[a] Emanuele Mauri,[a] Marta Moioli,[a] Andrea Mele,[a, b] and Maurizio Masi[a]

1. Introduction

The diffusion mechanism of solute molecules within hydrogels is historically of great interest for a wide variety of industrial applications, such as separations through membranes[1–4] and chromatographic columns.[5,6] Moreover, in recent years, diffusion studies applied to nanomedicine and, in particular, to hydrogels that are able to control and sustain the release of drugs have played a leading role.[7–10] Indeed several reports and reviews written recently, underline the importance of hydrogels in this field.[11–14] Hydrogels are cross-linked hydrophilic polymeric networks swollen in aqueous media, and are typically soft and elastic, owing to their thermodynamic compatibility with water.[15–17] Cross-links and interconnections, which bring polymer chains together, can be formed by physical entanglements, leading to physical hydrogels, or covalent bonds, leading to chemical ones.[15,18]

Hence, to improve the performance of materials in these fields, a deep understanding of solute diffusion in gel matrices is fundamental.[19–23] An examination of the literature provides both experimental studies and phenomenological theories related to the diffusion mechanism of molecules from macromolecular networks.[24–27] These theoretical descriptions can be classified into three main categories: 1) free-volume-based theories, which were originally developed for solute diffusion in pure liquids and extended the hole-hopping concept to polymeric systems; 2) hydrodynamic theories, which assume that polymer chains enhance the frictional drag on the solute by slowing down fluid flow in the proximity of the chains; and 3) obstruction theories, which describe polymer chains as an almost impenetrable network that increases the effective path length of diffusive transport.[28,29]

Despite all these proposals, the available data often show low or even no agreement with descriptive theories and, more generally, this topic is still greatly debated.[23,30–32] Indeed several studies on drug-delivery systems are centered on pure Fickian diffusion and also consider degradation (bulk or erosion) and swelling contributions.[33–35] However, especially at a drug concentration that is typical for pharmacological treatments, several other mechanisms, such as drug–polymer interactions, which could influence the mass transport, take place and cannot be neglected for optimal device design.[36–38]

Recently, experimental studies have been performed on adsorption associated with hydrogel delivery systems as a classic drug-loading process[39,40] and as a strategy to provide multiple drug-release rates,[41] but none of them considered a rationally derived model of adsorption. Here, we study the release of ethosuximide (ESM), a succinimide anticonvulsant commonly used in epilepsy,[42,43] through agar-carbomer-based hydrogels (AC), which have already been studied and characterized for central-nervous-system applications.[44–46] The choice of ESM was dictated by the following considerations: 1) In previous work,[33,47] we observed anomalous diffusion behavior for molecules carrying overall negative charges, such as sodium fluorescein (SF, double negative charge) and sodium ibuprofene (IP; single negative charge). In the present study, we considered a paradigmatic example of a neutral substrate to achieve more

[a] *Dr. F. Rossi,[+] Dr. F. Castiglione,[+] M. Ferro, P. Marchini, E. Mauri, M. Moioli, Prof. Dr. A. Mele, Prof. Dr. M. Masi*
Department of Chemistry
Materials and Chemical Engineering "Giulio Natta"
Politecnico di Milano, via Mancinelli 7, 20131 Milan (Italy)
Tel: (+39) 02 23993145
Fax: (+39) 02 23993180
E-mail: filippo.rossi@polimi.it

[b] *Prof. Dr. A. Mele*
CNR-ICRM, via Luigi Mancinelli 7
20131 Milan (Italy)

[+] *These authors equally contributed to this work.*

general conclusions. 2) We focused on low-molecular-weight molecules, as representatives of a large class of active pharmaceutical ingredients. 3) We focused on a molecule with a well-defined and simple NMR profile, in view of the NMR determination of the self-diffusion coefficients. Thus, when dealing with small molecules, two different approaches were followed to calculate ESM self-diffusion coefficients in the AC hydrogel. The first is an indirect and more traditional approach that is based on the in vitro study of release from the swollen hydrogels and the use of the data to calculate the self-diffusion coefficient by applying a mathematical understanding provided by classic Fick models. The second is a direct and strongly innovative approach, in which the ESM self-diffusion within gel matrices was measured by means of pulsed magnetic field gradients spin-echo (PGSE) nuclear magnetic resonance (NMR) spectroscopy, using the high resolution magic angle spinning (HR-MAS) technique.[2,47–49] Also, to understand the differences in terms of drug transport through water solutions and hydrogel environments, we propose here a mathematical model based on the adsorption mechanisms firstly applied by Carta and coworkers for polysaccharide-based hydrogels for chromatography[50] without fitted parameters to be predictive. The understanding of this additional phenomenon may pave to way to better device design with the possibility of predicting the release behavior by tuning materials properties, thus improving the chances of success in subsequent medical trials.

Experimental Section

Materials

Carbomer 974P (CAS 151687-96-6) with high molecular weight (about 1 MDa), was provided by Fagron (The Netherlands) and triethylamine (TEA; CAS 121-44-8) with high purity was purchased from Sigma–Aldrich (Germany). The solvent used was a phosphate buffer saline solution (PBS; Sigma–Aldrich, Germany). For spectroscopic analysis, deuterated PBS was used to avoid overlapping of the ^{1}H signal of ESM with those of PBS. The other polymer involved in the reaction is agarose (CAS 9012-36-6; Invitrogen, USA) and has a molecular weight of about 300 kDa. Ethosuximide (ESM; CAS 77-67-8) was purchased from Sigma–Aldrich (Germany). All materials were used as received.

Hydrogel Synthesis and Drug Loading

Carbomer 974P (0.05 g) was stirred in deuterated PBS (10 mL), and the resulting mixture was neutralized to pH 7.4 with TEA. Agarose powder (0.5% *w/v*) was subsequently added and the system was electromagnetically heated up to 80 °C to induce condensation reactions. ESM was added to the polymeric formulation as an aqueous solution, before the cross-linking procedure, and thus, sol/gel transition occurred; it was loaded in the range of 4–72 mg mL^{-1}, to explore the effects of concentration on transport properties. The gelling solution was then placed in steel cylinders (0.5 mL in each and each with the same dimensions of a standard well in a 48-cell culture plate) and left to rest at 37 °C until complete gelation and thermal equilibrium was reached. The formation of ester bonds between agarose and carbomer, which leads to the formation of hydrogel networks, has been described in previous reports, where we discussed the chemical nature of agarose-carbomer-based (AC) hydrogels.[51] As a result of these reactions, AC hydrogels are anionic; this electrostatic nature was confirmed by FT-IR and mass equilibrium swelling at different pHs.[52] For consistency, we will use the same acronyms for the hydrogels as used in previous studies.[53]

Transmission Electron Microscopy (TEM)

The AC hydrogel was swollen with a solution of $Pb(NO_3)_2$ to obtain suitable gels containing the contrast agent and sampled on a 300-mesh copper grid coated with a holey carbon film.[33] Images were recorded on a transmission electron microscope (Philips CM200 FEG) at an electron-accelerating potential of 200 kV.

ESM Release and Mathematical Modeling

Before carrying out release experiments, to avoid any interference with the mass-transfer processes owing to swelling phenomena, the hydrogel samples were left to swell until equilibrium was reached in the isoconcentrated ESM aqueous solution overnight. The degradation contribution can be neglected, as the characteristic time of release is much smaller than that of degradation, according with previous studies.[44,54] Three samples of gel loaded with an ESM concentration of 4 mg mL^{-1} were put in excess PBS (to maintain a constant pH of 7.4) and stored at 37 °C under a 5% CO_2 atmosphere. Minimal aliquots were collected at defined time points, while the solution was refreshed, to avoid mass-transfer equilibrium between the gel and the surrounding PBS solution, and thus, let the high concentration gradient be the driving force. A percentage of the ESM released was measured by UV spectroscopy at $\lambda = 254$ nm.[42] ESM diffusivity (D) was evaluated with a mathematical model based on mass balances, that is, on fundamental conservation laws.[54] Diffusion was described through the second Fick law with a 1D model in a cylindrical geometry, as shown in Equation (1). Here, the radius (r) is the characteristic dimension for the investigated transport phenomenon. Therefore, the abovementioned increase takes place owing to material flux, which takes place at the PBS/hydrogel surface [Eqs. (1)–(4)]. Equations (5) and (6) represent the boundary conditions for the left and the right border, respectively. Equation (5) implies profile symmetry at the center (that is, with respect to cylinder axis), whereas Equation (6) represents the equivalence between the material diffusive fluxes at the PBS/hydrogel surface.

$$\frac{\partial C_G}{\partial t} = D \cdot \frac{1}{r} \cdot \frac{\partial}{\partial r} \cdot \left(r \cdot \frac{\partial C_G}{\partial r} \right) \tag{1}$$

$$V_S \cdot \frac{\partial C_S}{\partial t} = k_C \cdot S_{exc} \cdot (C_G - C_S) \tag{2}$$

$$C_S(t = 0) = 0 \tag{3}$$

$$C_G(t = 0) = C_{G,0} = \frac{m_{G,0}}{V_G} \tag{4}$$

$$\left. \frac{\partial C_G}{\partial r} \right|_{r=0} = 0 \tag{5}$$

$$-D \cdot \left. \frac{\partial C_G}{\partial r} \right|_{r=R} = k_C \cdot (C_G - C_S) \tag{6}$$

The two mass balance equations involve the mean ESM concentration within the hydrogel (C_G), the mean ESM concentration in the outer solution (C_S), the volume of the solution (V_S), the hydrogel volume (V_G), the drug mass present inside the matrix (m_G) and the exchange interfacial surface (S_{exc}), that is, the boundary surface be-

tween gel and surrounding solution (which, by simplifying, can be here considered as being only the side surface). Finally, D represents the diffusion coefficient and k_C, the mass-transfer coefficient. The mass-transfer coefficient is computed through the Sherwood number (Sh) obtained by means of the penetration theory presented in Equation (7):[54]

$$Sh = \frac{8}{\pi} = \frac{k_C \cdot 2r}{D} \quad (7)$$

The (1)–(6) system was calculated numerically, assuming the constant gel dimensions, which is a reasonably valid assumption as degradation phenomena occur at a much slower rate than delivery, and because experiments were carried out on already gelled samples.

HR-MAS NMR spectroscopy

The ^{1}H NMR spectra of hydrogel systems were recorded on a Bruker Avance spectrometer operating at 500 MHz proton frequency, equipped with a dual ^{1}H/^{13}C high-resolution magic angle spinning (HR-MAS) probe head for semisolid samples. The basic principle of this approach can be summarized as follows. The fast rotation of the sample at the so-called magic angle (54.7° with respect to the z direction of the stray field of the NMR magnet) averages the dipole–dipole interactions and susceptibility distortions, causing a dramatic improvement of spectral resolution. Samples were transferred in a 4 mm ZrO_2 rotor containing a volume of about 12 μL. All the ^{1}H NMR spectra were acquired with a spinning rate of 4 kHz to eliminate the dipolar contribution. Self-diffusion coefficients were measured by diffusion-ordered correlation spectroscopy (DOSY) experiments, based on a PGSE approach. A pulsed gradient unit that was capable of producing magnetic-field pulse gradients in the z direction up to 53 G·cm^{-1} was used. These experiments were performed using the bipolar pulse longitudinal eddy current delay (BPPLED) pulse sequence. The duration of the magnetic-field pulse gradients (δ) and the diffusion times (Δ) were optimized for each sample to obtain complete dephasing of the signals with the maximum gradient strength. In each DOSY experiment, a series of 64 spectra with 32 k points were collected. For each experiment 32 scans were acquired. For the investigated samples, Δ was set to 0.1 s, whereas the δ values were in the range of 0.7–2 ms. The pulse gradients were increased from 2 to 95 % of the maximum gradient strength in a linear ramp. The temperature was set and controlled at 37 °C with an air flow of 535 L·h^{-1} to avoid any temperature fluctuations due to sample heating during the magnetic-field pulse gradients.

Adsorption Kinetics

Adsorption isotherms and batch uptake rates, obtained by material-balance and drug-concentration profiles of the gels were determined following literature methods.[50,55] In brief, the adsorption isotherms were obtained by suspending small gel samples in ESM solutions with different initial concentrations and mixing for 8 h.

Based on the kinetic measurements, this time was estimated to be sufficient to attain equilibrium even for the slowest resin considered. For the batch uptake rates, the agarose particles were suspended in a protein solution in an agitated vessel and the amount adsorbed was obtained from the residual drug concentration at each time.

Mathematical Model

The model discussed below, without fitted parameters, was developed with MatLab suite, using the *lsqcurvefit* function to match experimental data with the proposed physical chemical description.

Statistical Analysis

Where applicable, experimental data were analyzed using analysis of variance (ANOVA). Statistical significance was set to p value $<$ 0.05. Results are presented as the mean value $\pm$ standard deviation.

2. Results and Discussion

2.1. TEM Analysis

AC hydrogels were prepared through the chemical cross-linking of two polymers (agarose and carbomer 974P) by microwave-assisted polycondensation. Heating to 80 °C led to a higher macromer mobility, and thus, enhanced short-range interconnections among the functional groups of the polymers. Esterification, the main reaction, takes place between carbomer carboxy groups and the agarose hydroxy groups, to produce local networks also known as microgels. As polycondensation proceeds, the system's viscosity continuously increases, decreasing the probability of interactions between macromer reactive sites. Nevertheless, close functional groups still react efficiently, due to a slower mobility, but longer available reaction time. This physicochemical condition results in a "welding" between microgels surfaces, giving rise to the final 3D macrostructure. The cross-linking process during hydrogel synthesis produces a distribution of polymer-chain molecular weights between junctions and, correspondingly, a distribution of mesh sizes.[56,57] The 3D structure of a gel can be described as polymer chains interconnected to form meshes filled with an aqueous solution. Mesh size (ζ) describes the average distance between cross-links in the polymer network and can be estimated with Flory–Rehner theory.[56,58,59] The complete and exhaustive treatment of Flory–Rehner theory applied to AC hydrogels has been studied and presented previously.[51] The use of Flory–Rehner theory can be described as a first-approximation model to evaluate gel structural parameters, which deserve a deeper assessment. From this approximation we obtained mean values of mesh size (ζ), average molecular weight between two consecutive cross-links (M_C), cross-linking density (ν_e) ,and porosity (ε), as summarized in Table 1. In Figure 1, we present TEM analysis to show the nanostructure of the AC hydrogel; the image was recorded on samples stained with $Pb(NO_3)_2$ to achieve sufficient contrast.

Our results revealed that AC hydrogels possess a highly entangled structure; there are some bigger pores that contain small pores and some fibrillar networks on the pore walls. In addition, most of the pores are interconnected. The image (Figure 1) clearly illustrates the porous morphology of the material and the structural heterogeneities in the pore-size distribution; the mean mesh size value is around 50 nm. This value

Table 1. AC hydrogel structural parameters.

Parameters	AC
ζ [nm]	45 ± 8
M_C [g mol^{-1}]	2500 ± 250
ν_e [kmol cm^{-3}]	28 ± 3.2
ε [–]	0.9 ± 0.05

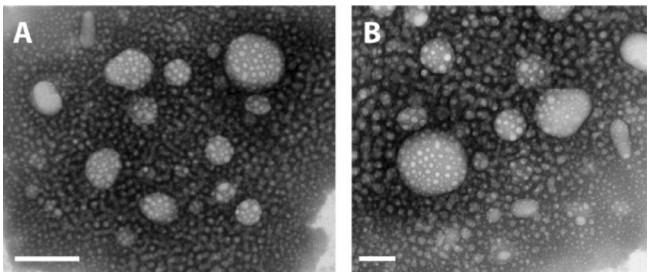

Figure 1. TEM images of the AC hydrogel. Scale bars: A) 100 nm. B) 50 nm.

is in complete accordance with the value calculated from Flory–Rehner theory and presented in previous studies.[51]

2.2. Drug Release

We loaded ESM into AC hydrogels and conducted a cumulative drug-release study in vitro to investigate the kinetics of drug release. ESM release profiles were measured in PBS at 37 °C once the gels had reached their swelling equilibrium. The data for ESM release are reported in Figure 2, where the cumulative mass fraction released into the surrounding solution is plotted against time. Figure 2 shows the sustained release of ESM in PBS over 24 h. ESM release seems to be driven by Fickian diffusion with only a small burst effect. In accordance with drug-delivery literature, "burst release" refers to the initial release of a large bolus of drug before the release rate reaches a stable profile.[60] It is usually caused by: 1) drug molecules that are at or near the solvent-hydrogel interface, and thus, can rapidly penetrate the supernatant solution and 2) drug molecules that find a fast path through large pores of the hydrogel, in contrast to those that diffuse through smaller pores, thus partially suffering from constrained molecular motion. After the initial small burst, the release became slower and is mainly mediated by Fickian diffusion.[61,62]

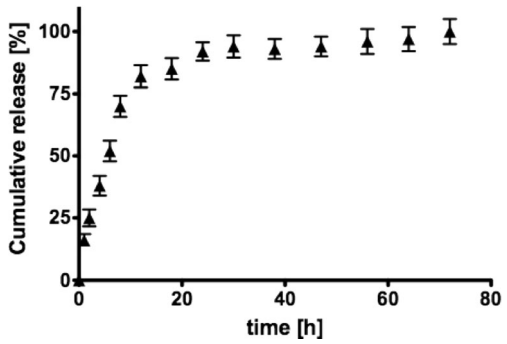

Figure 2. ESM release from AC hydrogels. Values are calculated as a percentage of the total mass loaded (mean value ± standard deviation are plotted).

Release data were used to estimate the ESM mass-transfer and diffusion coefficients in the AC hydrogel. The numeric values are: $k_C = (2.84 \pm 0.2) \times 10^{-7}$ m s^{-1} and $D = (1.11 \pm 0.12) \times 10^{-9}$ m^2 s^{-1}, where k_C is the mass-transfer coefficient and D is the diffusion coefficient calculated according to the theoretical approach described above. In Fickian diffusion theory, D is assumed to be a constant material property and so this value is representative of all solute concentrations (inside the solubility range).

Moreover, several problems are connected with this indirect measurement of diffusivity, which often contains a large number of errors. Indeed performing release studies with hydrogels, as soft matter, is quite difficult, because we must be sure of the integrity of the system, avoid hydrogel destruction during water changes, be confident about the complete absence of residual drug molecules after water changes, and maintain the concentration gradient.

In addition, we must be sure of the detection range (typical for each molecule), avoiding high or low concentrations, which are not detectable due to saturation and instrumental problems, respectively. In brief, the main concern is to not introduce artifacts in the releasing system. In this direction, the research community is moving toward the use of direct and independent diffusivity measurements to avoid all these issues.[2,63,64] Despite the fact that concentration-gradient diffusivity and self-diffusivity present some differences, the literature has provided several correlations[23,65] to relate them. These correlations take into account the hindered contribution of hydrogels in terms of porosity and tortuosity, underlining that the two values are in good agreement if we consider small molecules within bigger pores.[23]

2.3 Experimental Measurement of Diffusion Coefficients through HR-MAS NMR Technique

The ^{1}H NMR spectrum of AC hydrogels is characterized by broad signals due to the residual solid-state effects related to dipole–dipole coupling. This shortcoming makes the NMR spectra acquired by conventional liquid-state probe heads completely useless for the structural and dynamical characterization of the materials.[7] The use of HR-MAS allowed us to overcome this limitation.[47,48]

The HR-MAS NMR methodology opened the possibility of using the whole repertoire of high-resolution NMR pulse sequences to investigate semisolid materials, including heterogeneous systems, ex vivo medical specimens, and soft matter. In the present study, the use of HR-MAS NMR together with the a PGSE pulse sequence offered the unique opportunity to measure the self-diffusion coefficient of the entrapped molecules (ESM) within the gel matrix, thus providing experimental data that reflects the transport properties of the encapsulated molecule in its real environment. The ^{1}H HR-MAS NMR spectrum of ESM dissolved in AC hydrogel is shown in Figure 3 to-

gether with peak assignments; the molecular formula of ESM and the atom numbering are also shown.

ESM diffusivity was measured at different concentrations both in the gel and in water, to study and understand the differences due to the environment of diffusion. As shown in Table 2, the diffusion coefficient of ESM in D_2O decreases from $(0.92 \pm 0.05) \times 10^{-9}$ to $(0.78 \pm 0.05) \times 10^{-9}\ m^2 s^{-1}$, thus indicating aggregation to larger molecular associations in highly concentrated solutions. The data for the D_2O solution of ESM were used as a reference for comparison with the homologues obtained from gel experiments, allowing the evaluation of the hydrogel effect on diffusivity.

The values shown in Table 2 point to the counterintuitive finding that ESM diffusivity in gels increases with increasing concentration from $(0.49 \pm 0.03) \times 10^{-9}$ to $(0.87 \pm 0.05) \times 10^{-9}\ m^2 s^{-1}$. This behavior is the opposite to that observed in D_2O, thus indicating that the molecular environment of the diffusing species might dramatically influence the transport phenomena.

The increasing diffusivity of ESM with increasing concentration should be considered and understood to enable better device design. Fickian diffusion itself is indeed not able to reproduce the results obtained at a low ESM concentration of $C_G = 4\ mg\,mL^{-1}$, which is representative of the values used in clinical studies. Indeed, recent and successful studies of in vivo applications of ESM released from hydrogels in epilepsy carried out by Hsiao and co-workers,[43] revealed a high efficacy for ESM at a concentration of $1.33\ mg\,mL^{-1}$. The in vivo study of Huang and co-workers,[66] showed a significant reduction in the spike-wave discharge during epileptic seizures for an ESM concentration of approximately $1.5\ mg\,mL^{-1}$.

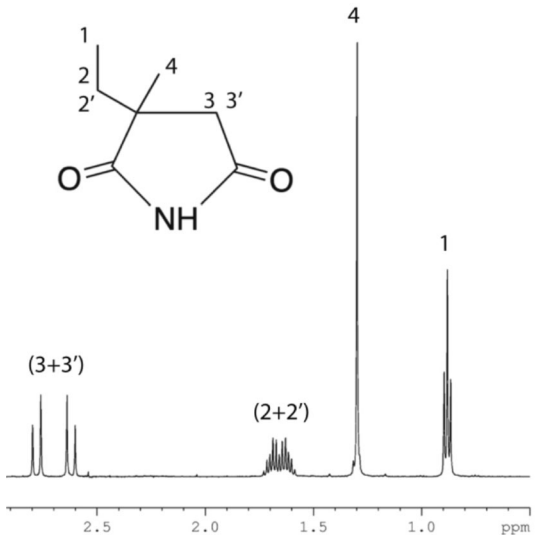

Figure 3. Molecular structure of ESM and ^1H HR-MAS NMR spectrum of ESM loaded within AC hydrogel ($75\ mg\,mL^{-1}$) together with peak assignment.

Table 2. Diffusion coefficients of ESM at different concentrations in: water solution (D_0), in AC hydrogel (D) and their ratio (D/D_0).

ESM concentration [$mg\,mL^{-1}$]	Da $m^2 s^{-1}$]	D_0[a] [$m^2 s^{-1}$]	D/D_0
4	0.49 ± 0.03	0.92 ± 0.05	0.53 ± 0.05
19	0.87 ± 0.05	0.88 ± 0.05	0.99 ± 0.08
38	0.89 ± 0.05	0.86 ± 0.05	1.03 ± 0.08
56	0.91 ± 0.06	0.82 ± 0.05	1.11 ± 0.1
75	0.87 ± 0.05	0.78 ± 0.05	1.11 ± 0.12

[a] All values have to be multiplied by 10^{-9}.

2.4. Modeling ESM Diffusion Coefficients in AC Hydrogels

As shown earlier, with data from drug-release experiments the Fick model is not able to provide reliable diffusion coefficients for low concentrations of ESM. The mismatch observed above cannot be solved by only considering classic Fick models, we should introduce other mechanisms. The increasing trend of gel diffusivity, indeed, reveals that in this case concentration-dependent mass transport is occurring.[67]

Here, drug motion within the pores is also influenced by the environment and, in particular, drug–polymer interactions. We propose a model that is able to describe the experimental behavior based on the following hypotheses. At low ESM concentration, the dominant feature is the adsorption of ESM within the hydrogel pores and, in accordance with Table 2, the diffusivity in the gel is lower than the diffusivity in water. As the adsorption sites are progressively saturated, ESM is then able to diffuse faster, with rates that are comparable to those observed in the water environment and are only driven by the concentration gradient. This is consistent with the fact that the mean gel-network mesh size (Figure 1) is much larger than the mean hydrodynamic radius of ESM. As a consequence, the ESM molecules inside the entangled hydrogel network show a mobility that is similar to that observed in D_2O solution, and thus, undergo diffusion with a high free motion. A pictorial representation of the conceptual model is shown in Figure 4, where the solid lines represent the agarose matrix, black circles represent the ESM molecules adsorbed onto the network backbone (black), and unfilled circles represent ESM molecules free to move within the network (white). From an experimental point of view, the NMR spectrum (see Figure 3) does not show the adsorbed and free species, but rather indicates that the exchange between those two states is fast on the NMR timescale. Consequently, the data obtained by PGSE-NMR experiments

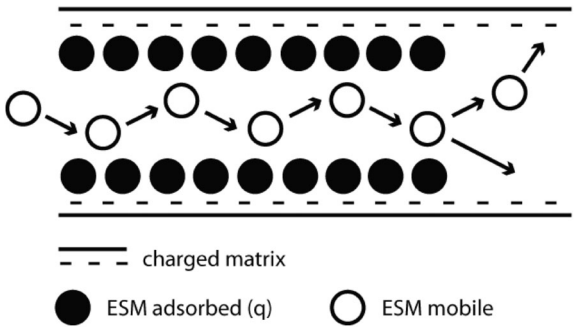

Figure 4. Pictorial representation of the partitioning model.

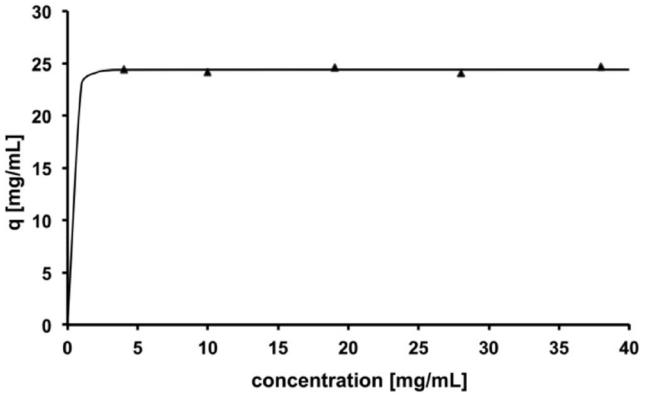

Figure 5. Adsorption isotherm for ESM on AC hydrogel. The line is based on Equation (8).

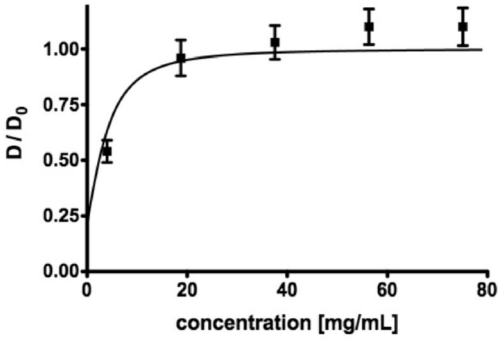

Figure 6. Comparison of model prediction (line) to HR-MAS data (dots) of ESM normalized diffusivity (D/D_0) within the AC hydrogel. The curve represents the trend predicted by Equation (10). Each data point is an average and the error bars represent standard deviations.

are the weighted average of both the adsorbed and free diffusion rates.

A mathematical model accounting for such mechanism may be proposed as follows. The adsorbed amount of ESM within hydrogel pores is given by q, as determined from the adsorption Langmuir isotherm (Figure 5). The isotherm is highly favorable at low drug concentrations. Thus, a Langmuir isotherm was used to fit the data according to Equation (8):

$$q = \frac{q^{\infty} \cdot K \cdot C_G}{1 + K \cdot C_G} \tag{8}$$

where q^{∞} is the maximum total adsorbed concentration of ESM and C_G is the ESM concentration within the hydrogel. The fitted line is presented in Figure 5 and calculated parameters are: $q^{\infty} = 25\ \mathrm{mg\,cm^{-3}}$ and $K = 302\ \mathrm{cm^3\,mg^{-1}}$. Adsorption parameters were used to modify the classic Fick law by considering that: 1) only molecules not adsorbed are available and could diffuse through the network and 2) porosity (ε) influences adsorption. In this direction, Equation (9) takes into account both the diffusion and the adsorption contribution:

$$\varepsilon \cdot \frac{\partial C_G}{\partial t} = \varepsilon \cdot D \cdot \frac{\partial^2 C_G}{\partial \chi^2} - (1 - \varepsilon) \cdot \frac{\partial q}{\partial t} \tag{9}$$

where ε is the gel porosity calculated in previous works[7] and C_G is ESM concentration within the hydrogel. From Equation (9) we can easy obtain the D/D_0 ratio [Eq. (10)]:

$$\frac{D}{D_0} = \frac{\varepsilon}{\varepsilon + (1 - \varepsilon) \cdot \frac{q^{\infty} \cdot K}{(1 + K \cdot C_G)^2}} \tag{10}$$

The results of the model developed, compared with the experimental values previously presented in Table 2, are presented in Figure 6. The good agreement between model (line) and experiments (ν) underlines that the adsorption isotherm together with diffusion through pores can describe the mechanisms involved in ESM release from a 3D polymeric network. In particular: 1) The drug is first partitioned and adsorbed into the hydrogel pores. The amount of adsorbed drug is given by q^{∞}, which is determined from the adsorption isotherm. Here, the adsorption mechanism prevails and the ESM diffusivity within the hydrogel is lower than in water. 2) At higher ESM concentration all adsorption sites are saturated and transport occurs by diffusion with a driving force determined by the ESM concentration gradient. 3) The effective diffusion coefficient in the pores determined with HR-MAS is constant and it is expected to be similar to that determined from NMR experiments in water solutions (see Table 2). So, adsorption is fundamental and cannot be neglected at ESM concentrations that are typical in clinical studies (described above), whereas it seems to be less important at higher drug concentrations.

The data summarized in Figure 6 could be considered as a starting point to investigate other scenarios to understand the release mechanism with the aim of controlling and tuning the release rates of ESM. In Figure 7, the dependence of diffusivity in gel on hydrogel porosity (ε) is presented.

The adsorption kinetics becomes slower as gel porosity decreases and consequently the adsorption contribution. In particular, at ESM concentrations at which the adsorption mechanism is not negligible, the concentration increases with decreasing porosity.

To investigate the role of cross-linkers in ESM transport we compared the results obtained with the AC hydrogel, already plotted in Figure 6, with D/D_0 values acquired with hydrogel

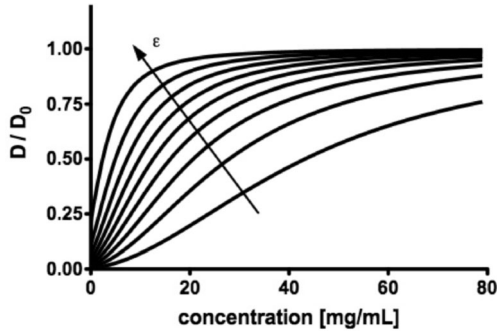

Figure 7. Simulations of ESM normalized diffusivity (D/D_0) tuning hydrogel porosity (ε).

AC6, characterized by a mean mesh size (ζ) that is equal to 7 nm, as previously reported along with the complete synthesis and characterization (Figure 8).[7,47] With increasing ESM concentration the ratio between diffusivity in hydrogel environment and diffusivity obtained in water solution increases. This is consistent with the data obtained for the AC hydrogel (Figure 6). Moreover, the importance of the adsorption mechanism grows as the mean mesh size decreases. Indeed, also at higher ESM concentrations in the case of AC6, we do not obtain results comparable with the AC hydrogel and ESM moves slower within the polymeric network.

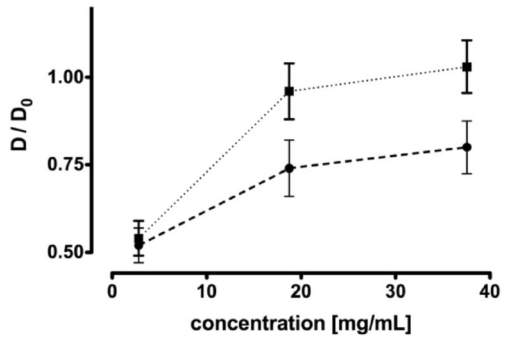

Figure 8. Diffusion normalized coefficients (D/D_0) for hydrogels AC ($\zeta = 45$ nm, ■) and AC6 ($\zeta = 7$ nm, ●) at different ESM concentrations.

In particular, at lower mean mesh size the adsorption is present also at higher ESM concentration and so cannot be neglected in drug-transport rationalization; the lower the mesh size, the higher the adsorption contribution.

3. Conclusions

A current trend in the field of controlled drug delivery is the development of multicomponent material systems, that is, the integration of multiple materials with diverse physicochemical properties. To better elucidate drug-transport mechanisms and predict transport behavior, it is crucial to correctly establish the connection between measurements at a molecular level and drug-release kinetics. The present work has given a deeper insight into the transport behavior of ESM, a commonly used anticonvulsant, within polymeric matrices by using a simple mathematical model.

The purpose of such modeling, as mentioned, was to provide a simple, but powerful tool to understand the influence of the design parameters on drug transport; this also allows the design of smart devices, for which the final product is tailored according to the specific needs.

This model successfully predicted the experimental trends at drug concentrations that are typical of clinical studies and at which the adsorption contribution is important and cannot be neglected, due to the consequent slower motion in the gel than in water.

At higher the drug concentrations, at which all adsorption sites were saturated, drug motion was less influenced by adsorption and diffusion remained the key transport mechanism. Moreover, the influence of adsorption seems to be related to mean mesh size: the smaller the pores, the higher the adsorption contribution. Hence, from the point of view of applications, it is possible to optimize the experimental activity, which can be expensive and time consuming, through a model-driven experimental approach, thus avoiding the classic trial-and-error modus operandi. A more careful management of resources is required nowadays in all research and development activities.

[1] D. E. Liu, C. Kotsmar, F. Nguyen, T. Sells, N. O. Taylor, J. M. Prausnitz, C. J. Radke, *Ind. Eng. Chem. Res.* **2013**, *52*, 18109 – 18120.
[2] J. E. Jenkins, M. R. Hibbs, T. M. Alam, *ACS Macro Lett.* **2012**, *1*, 910 – 914.
[3] Q. Wu, Y. Sun, H. Bai, G. Shi, *Phys. Chem. Chem. Phys.* **2011**, *13*, 11193 – 11198.
[4] Y. Y. Liang, L. M. Zhang, W. Jiang, W. Li, *ChemPhysChem* **2007**, *8*, 2367 – 2372.
[5] J. E. Basconi, G. Carta, M. R. Shirts, *AIChE J.* **2014**, *60*, 3888 – 3901.
[6] R. K. Lewus, G. Carta, *Ind. Eng. Chem. Res.* **2001**, *40*, 1548 – 1558.
[7] M. Santoro, P. Marchetti, F. Rossi, G. Perale, F. Castiglione, A. Mele, M. Masi, *J. Phys. Chem. B* **2011**, *115*, 2503 – 2510.
[8] F. Brandl, F. Kastner, R. M. Gschwind, T. Blunk, J. Tessmar, A. Gopferich, *J. Controlled Release* **2010**, *142*, 221 – 228.
[9] C. Kotsmar, T. Sells, N. Taylor, D. E. Liu, J. M. Prausnitz, C. J. Radke, *Macromolecules* **2012**, *45*, 9177 – 9187.
[10] E. Verheyen, S. van der Wal, H. Deschout, K. Braeckmans, S. de Smedt, A. Barendregt, W. E. Hennink, C. F. van Nostrum, *J. Controlled Release* **2011**, *156*, 329 – 336.
[11] L. A. Sharpe, A. M. Daily, S. D. Horava, N. A. Peppas, *Expert Opin. Drug Delivery* **2014**, *11*, 901 – 915.
[12] F. Rossi, G. Perale, S. Papa, G. Forloni, P. Veglianese, *Expert Opin. Drug Delivery* **2013**, *10*, 385 – 396.
[13] J. X. Cui, D. P. Wang, K. Koynov, A. del Campo, *ChemPhysChem* **2013**, *14*, 2932 – 2938.
[14] G. B. Demirel, R. von Klitzing, *ChemPhysChem* **2013**, *14*, 2833 – 2840.
[15] B. V. Slaughter, S. S. Khurshid, O. Z. Fisher, A. Khademhosseini, N. A. Peppas, *Adv. Mater.* **2009**, *21*, 3307 – 3329.
[16] R. Langer, *Adv. Mater.* **2009**, *21*, 3235 – 3236.
[17] N. Annabi, A. Tamayol, J. A. Uquillas, M. Akbari, L. E. Bertassoni, C. Cha, G. Camci-Unal, M. R. Dokmeci, N. A. Peppas, A. Khademhosseini, *Adv. Mater.* **2014**, *26*, 85 – 124.
[18] E. S. Dragan, *Chem. Eng. J.* **2014**, *243*, 572 – 590.
[19] S. Lehmann, S. Seiffert, W. Richtering, *J. Am. Chem. Soc.* **2012**, *134*, 15963 – 15969.
[20] B. Amsden, *Macromolecules* **1998**, *31*, 8382 – 8395.
[21] J. Siepmann, N. A. Peppas, *Adv. Drug Delivery Rev.* **2001**, *48*, 139 – 157.
[22] J. Siepmann, K. Siepmann, *Int. J. Pharm.* **2008**, *364*, 328 – 343.
[23] J. Kärger, *ChemPhysChem* **2015**, *16*, 24 – 51.
[24] G. G. Ferrer, M. M. Pradas, J. L. G. Ribelles, F. R. Colomer, I. Castilla-Cortazar, A. Vidaurre, *Eur. Polym. J.* **2010**, *46*, 774 – 782.
[25] K. Lebedev, S. Mafe, P. Stroeve, *J. Colloid Interface Sci.* **2006**, *296*, 527 – 537.
[26] K. Vulic, M. M. Pakulska, R. Sonthalia, A. Ramachandran, M. S. Shoichet, *J. Controlled Release* **2015**, *197*, 69 – 77.
[27] D. Caccavo, S. Cascone, G. Lamberti, A. A. Barba, *Mol. Pharm.* **2015**, *12*, 474 – 483.
[28] S. Seiffert, J. Sprakel, *Chem. Soc. Rev.* **2012**, *41*, 909 – 930.
[29] B. Amsden, *Macromolecules* **2001**, *34*, 1430 – 1435.
[30] L. Masaro, X. X. Zhu, *Prog. Polym. Sci.* **1999**, *24*, 731 – 775.
[31] I. Kohli, A. Mukhopadhyay, *Macromolecules* **2012**, *45*, 6143 – 6149.
[32] N. A. Hadjiev, B. Amsden, *J. Controlled Release* **2015**, *199*, 10 – 16.
[33] M. Ferro, F. Castiglione, C. Punta, L. Melone, W. Panzeri, B. Rossi, F. Trotta, A. Mele, *Beilstein J. Org. Chem.* **2014**, *10*, 2715 – 2723.
[34] Y. Fu, W. J. Kao, *Expert Opin. Drug Delivery* **2010**, *7*, 429 – 444.

[35] G. Lamberti, I. Galdi, A. A. Barba, *Int. J. Pharm.* **2011**, *407*, 78 – 86.
[36] V. Hagel, T. Haraszti, H. Boehm, *Biointerphases* **2013**, *8*, 36.
[37] J. Cleary, L. E. Bromberg, E. Magner, *Langmuir* **2003**, *19*, 9162 – 9172.
[38] P. C. Griffiths, P. Stilbs, A. M. Howe, T. H. Whitesides, *Langmuir* **1996**, *12*, 5302 – 5306.
[39] C. Alvarez-Lorenzo, A. Concheiro, *J. Controlled Release* **2002**, *80*, 247 – 257.
[40] M. F. A. Taleb, S. E. Abdel-Aal, N. A. El-Kelesh, E. S. A. Hegazy, *Eur. Polym. J.* **2007**, *43*, 468 – 477.
[41] B. Yu, X. S. Jiang, J. Yin, *Macromol. Chem. Phys.* **2014**, *215*, 2283 – 2294.
[42] W. C. Huang, T. J. Lee, C. S. Hsiao, S. Y. Chen, D. M. Liu, *J. Mater. Chem.* **2011**, *21*, 16077 – 16085.
[43] M. H. Hsiao, M. Larsson, A. Larsson, H. Evenbratt, Y. Y. Chen, Y. Y. Chen, D. M. Liu, *J. Controlled Release* **2012**, *161*, 942 – 948.
[44] G. Perale, F. Rossi, M. Santoro, M. Peviani, S. Papa, D. Llupi, P. Torriani, E. Micotti, S. Previdi, L. Cervo, E. Sundstrom, A. R. Boccaccini, M. Masi, G. Forloni, P. Veglianese, *J. Controlled Release* **2012**, *159*, 271 – 280.
[45] S. Papa, F. Rossi, R. Ferrari, A. Mariani, M. De Paola, I. Caron, F. Fiordaliso, C. Bisighini, E. Sammali, C. Colombo, M. Gobbi, M. Canovi, J. Lucchetti, M. Peviani, M. Morbidelli, G. Forloni, G. Perale, D. Moscatelli, P. Veglianese, *ACS Nano* **2013**, *7*, 9881 – 9895.
[46] S. Papa, R. Ferrari, M. De Paola, F. Rossi, A. Mariani, I. Caron, E. Sammali, M. Peviani, V. Dell'Oro, C. Colombo, M. Morbidelli, G. Forloni, G. Perale, D. Moscatelli, P. Veglianese, *J. Controlled Release* **2014**, *174*, 15 – 26.
[47] G. Perale, F. Rossi, M. Santoro, P. Marchetti, A. Mele, F. Castiglione, E. Raffa, M. Masi, *J. Biomed. Nanotechnol.* **2011**, *7*, 476 – 481.
[48] T. M. Alam, M. R. Hibbs, *Macromolecules* **2014**, *47*, 1073 – 1084.
[49] A. Mele, F. Castiglione, L. Malpezzi, F. Ganazzoli, G. Raffaini, F. Trotta, B. Rossi, A. Fontana, G. Giunchi, *J. Inclusion Phenom. Macrocyclic Chem.* **2011**, *69*, 403 – 409.
[50] E. B. Schirmer, G. Carta, *AIChE J.* **2009**, *55*, 331 – 341.
[51] F. Rossi, G. Perale, G. Storti, M. Masi, *J. Appl. Polym. Sci.* **2012**, *123*, 2211 – 2221.
[52] F. Rossi, G. Perale, M. Masi, *Chem. Pap.* **2010**, *64*, 573 – 578.
[53] F. Rossi, M. Santoro, T. Casalini, P. Veglianese, M. Masi, G. Perale, *Int. J. Mol. Sci.* **2011**, *12*, 3394 – 3408
[54] F. Rossi, R. Ferrari, S. Papa, D. Moscatelli, T. Casalini, G. Forloni, G. Perale, P. Veglianese, *Colloids Surf. B* **2013**, *108*, 169 – 177.
[55] E. B. Schirmer, G. Carta, *AIChE J.* **2007**, *53*, 1472 – 1482.
[56] L. Pescosolido, L. Feruglio, R. Farra, S. Fiorentino, I. Colombo, T. Coviello, P. Matricardi, W. E. Hennink, T. Vermonden, M. Grassi, *Soft Matter* **2012**, *8*, 7708 – 7715.
[57] M. Wallace, D. J. Adams, J. A. Iggo, *Soft Matter* **2013**, *9*, 5483 – 5491.
[58] P. J. Flory, *Principles of polymer chemistry*, Cornell University Press, New York, **1953**.
[59] S. J. de Jong, B. van Eerdenbrugh, C. F. van Nostrum, J. J. Kettenes-van de Bosch, W. E. Hennink, *J. Controlled Release* **2001**, *71*, 261 – 275.
[60] X. Huang, C. S. Brazel, *J. Controlled Release* **2001**, *73*, 121 – 136.
[61] K. Vulic, M. S. Shoichet, *J. Am. Chem. Soc.* **2012**, *134*, 882 – 885.
[62] P. L. Ritger, N. A. Peppas, *J. Controlled Release* **1987**, *5*, 23 – 36.
[63] S. Matsukawa, H. Yasunaga, C. Zhao, S. Kuroki, H. Kurosu, I. Ando, *Prog. Polym. Sci.* **1999**, *24*, 995 – 1044.
[64] D. Bernin, G. J. Goudappel, M. van Ruijven, A. Altskar, A. Strom, M. Rudemo, A. M. Hermansson, M. Nyden, *Soft Matter* **2011**, *7*, 5711 – 5716.
[65] M. A. Gagnon, M. Lafleur, *J. Phys. Chem. B* **2009**, *113*, 9084 – 9091.
[66] H. Y. Huang, S. H. Hu, C. S. Chian, S. Y. Chen, H. Y. Lai, Y. Y. Chen, *J. Mater. Chem.* **2012**, *22*, 8566 – 8573.
[67] N. F. E. I. Nestle, R. Kimmich, *J. Phys. Chem.* **1996**, *100*, 12569 – 12573.